ENG. Struct. Civ. Eng. 2026, 20(10): 1871–1889
https://doi.org/10.1007/s11709-026-1350-4

REVIEW

Printcrete: Upgrading shotcrete

Yong YUAN[a], Jiao-Long ZHANG[a], Yaxin TAO[a,b*]

[a] *Department of Geotechnical Engineering, Tongji University, Shanghai 200092, China*
[b] *Institute for Building Materials, ETH Zürich, Zürich 8093, Switzerland*
[*] *Corresponding author. E-mail: taoyaxin@tongji.edu.cn*

© The Author(s) 2026. This article is published with open access at link.springer.com and journal.hep.com.cn

ABSTRACT Printable concrete (hereafter printcrete) is a promising additive construction technology and a novel alternative to conventional shotcrete for tunnel engineering, offering advantages such as eliminating rebound and enhancing flexibility. Despite its potential, challenges remain in upscaling, performance, and applicable equipment. This paper consolidates the prior research on printcrete carried out by the authors, while also offering insights into the advancement of printcrete technology from both sustainable and intelligent perspectives. It begins by addressing the mixture design at both the concrete and paste levels to reduce the carbon footprint of printcrete. The advantages of incorporating coarse aggregates in reducing binder content, along with the associated challenges in processing, are discussed. Additionally, various reaction mechanisms based on low-carbon, fast-setting binders, such as aluminate-based cement and other supplementary cementitious materials, have been studied for printcrete, enabling the decoupling of productive strength from service strength to improve its sustainability. Based on these reaction mechanisms, a twin-pipe pumping technology has been developed to balance the conflicting requirements of pumpability and buildability. This highlights the need for novel indices and standardized testing methods to characterize the early-age hydration and rheological evolution, addressing the accurate time-dependent demands of printcrete. Lastly, a detailed discussion on smart construction is presented, emphasizing its importance in extreme environments, where automated equipment integrated with artificial intelligence is essential for real-time monitoring and adaptive decision-making.

KEYWORDS printcrete, tunneling engineering, concrete processing, low-carbon materials, smart construction

1 Introduction

The use of concrete as a building material dates back millennia, with its widespread adoption in modern construction primarily due to its durability, versatility, and cost-effectiveness. However, conventional concreting methods present several limitations, especially those involving formwork. Formwork construction is labor-intensive, time-consuming, and often leads to significant material waste. Moreover, creating complex architectural forms requires custom formwork, which is both expensive and resource-intensive. These limitations have driven the search for more efficient and sustainable construction methods, leading to the development of printable concrete as additive manufacturing in construction, hereafter referred to as printcrete [1].

Printcrete offers a paradigm shift by enabling the direct extrusion of concrete into predefined shapes without the need for supporting formwork. This approach not only reduces the material waste associated with formwork but also opens new possibilities for architectural and structural design with complex geometries [2]. Furthermore, printcrete has the potential to significantly reduce construction times, as the need for formwork assembly and disassembly is eliminated. In addition to that, printcrete can also be used in cases where formwork is unachievable. One representative application for printcrete is tunnel construction, which could potentially replace or complement existing technologies such as shotcrete (Fig. 1) [3].

Despite the widespread use of shotcrete, several notable drawbacks still exist. One of the primary issues with shotcrete is the phenomenon of rebound. Reported rebound rates vary widely: typically 30%–40% for dry-mix and 5%–15% for wet-mix shotcrete [4]. This not only leads to material wastage but also creates a hazardous

Article history: Received Aug 16, 2025; Accepted Jan 7, 2026

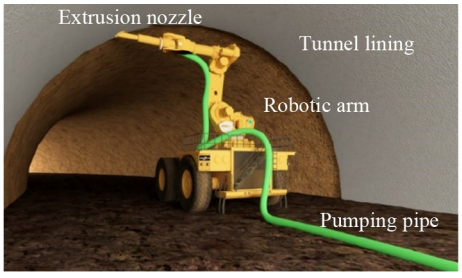


Fig. 1 Schematic of printcrete for tunneling engineering. The material is pumped through a delivery pipe and extruded via a nozzle. The precise movement of a robotic arm ensures accurate placement, allowing the concrete to form tunnel linings.

working environment by generating dust and debris. Moreover, the rebound material is often difficult to recover and reuse, contributing to resource inefficiency. In addition to rebound, shotcrete has limitations in terms of the precision and quality of the final structure. The high velocity of the sprayed concrete can result in uneven surfaces and poor control over the thickness of the applied layer, leading to variability in structural performance.

Considering the limitations of shotcrete, there is a clear need for alternative technologies to address these issues while maintaining or improving the efficiency and effectiveness of tunneling operations. Printcrete presents a promising alternative with its ability to control material deposition and create structures precisely without rebound. Unlike shotcrete, printcrete allows for the controlled extrusion of concrete layer by layer, enabling the construction of highly detailed and complex structures with minimal material waste [5]. However, the adoption of printcrete in tunnel engineering is not without challenges, particularly in terms of material properties, equipment requirements, and the long-term performance of printed structures. These factors are critical to the performance and applicability of printcrete in tunneling engineering, where the structural demands and environmental conditions are often more severe than those encountered in above-ground construction.

To address these issues, the primary objective of this paper is to critically review and consolidate current advances in printcrete technology with a specific focus on its application in tunnel engineering. The final goal is to support the development of reliable, sustainable, and automated three-dimensional (3D) printing solutions for tunnel construction. Specifically, this paper is structured as follows. Section 2 begins with an exploration of the printcrete mixture, emphasizing the development of sustainable materials at both the concrete and paste levels. Next, Section 3 delves into the required performance characteristics of printcrete, which are critical at different stages of the production and construction processes, including pumpability, extrudability, buildability, and structural ability. After that, Section 4 examines methods for measuring these performance characteristics, covering rheological measurements and the quantification of interfacial adhesion. Section 5 discusses the equipment necessary for printcrete applications, including mixers, pumps, nozzles, and curing devices, highlighting the advancements in innovative, intelligent, real-time controlling techniques used throughout the process. Finally, the paper concludes with future research and development recommendations, aiming to advance printcrete technology and expand its use in sustainable and intelligent tunnel construction.

2 Mixture design of printcrete

One of the key challenges associated with printcrete is enhancing its sustainability. Three key strategies to reduce cement usage can be considered to improve sustainability: reducing the amount of concrete used in structures, decreasing the paste content within the concrete, and optimizing the binder content in the paste. For tunnel lining applications, reducing concrete usage by optimizing the structural configuration is often limited due to functional and structural constraints. Therefore, an alternative approach is to adopt a higher strength grade of concrete. In this context, matrix design becomes critical and should focus on optimizing the mixture components at the concrete level and the cement content at the paste level.

2.1 Design from a concrete level

Most mixtures currently used for printing concrete are more accurately described as mortars rather than true concrete. This distinction arises from the absence of coarse aggregates in most printable mixtures. While there have been efforts by researchers to develop real printable concrete [6], a form of concrete that includes coarse aggregates, these mixtures still differ significantly from traditional pumpable and cast concretes in terms of aggregate content and size. This means that the binder content in printcrete is much higher than that of conventional concrete, thus leading to major sustainability concerns (Fig. 2). Mohan et al. [9] conducted a comprehensive review highlighting this discrepancy, noting that the binder content in printcrete mixtures often exceeds 800 kg/m^3, significantly higher than the approximately 350 kg/m^3 binder content typical of conventional cast concrete and shotcrete. This elevated binder content is primarily driven by the need to enhance workability and maintain a stable flow during the extrusion process, which is crucial for higher productivity in printcrete applications. However, this trade-off between sustainability and productivity remains a significant challenge.

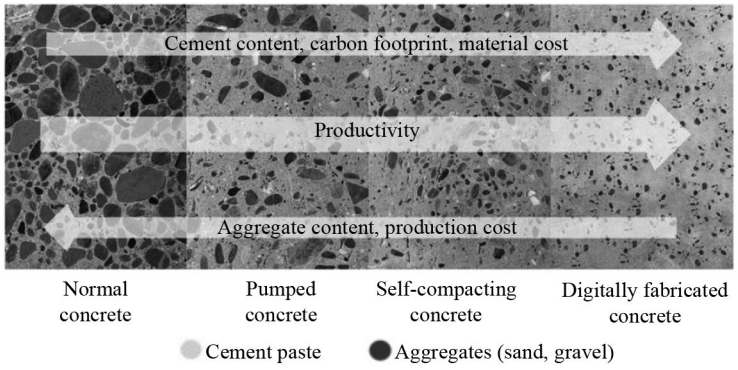


Fig. 2 Relationship between aggregate content and productivity-enhancing technologies. Digitally fabricated concrete refers to printcrete. Reprinted from Refs. [7,8].

One potential approach to addressing this challenge is to optimize the mixture design by maximizing the packing fraction of aggregates [10]. By optimizing the aggregate grading to achieve the maximum packing fraction, it is possible to reduce the amount of binder required to fill the voids between aggregates, thereby lowering the overall binder content. However, optimizing the packing fraction must be carefully balanced with the processing requirements of printcrete. The mixture must still possess adequate flowability and cohesion to be extruded smoothly through the nozzle without clogging and to maintain the shape integrity of printed layers.

The use of manufactured aggregates has been investigated as a substitute for natural sand in concrete mixtures, including those intended for printing to address sustainability issues. The angular shape of manufactured aggregates improves particle interlocking, thereby increasing the shape stability of printcrete, as proved by Tao et al. [11]. However, the use of angular aggregates may also introduce drawbacks such as increased bleeding risk or reduced extrudability, due to their irregular surface texture and higher surface area, which can interfere with paste coating and lubrication. In addition, the on-site utilization of tunnel-excavated materials presents another promising approach to enhancing the sustainability of printcrete. Several studies have investigated the feasibility of using tunnel-excavated materials as aggregates in shotcrete and tunnel lining concrete, demonstrating the required mechanical performance and notable environmental advantages [12]. However, a significant challenge lies in the quality variability of aggregates derived from tunnel-excavated materials, which is highly dependent on the geological characteristics of the source rock.

2.2 Design from a paste level

This section focuses on the reaction mechanisms crucial for understanding printcrete, particularly in meeting various performance requirements (as outlined in Section 3) and system design considerations (as described in Section 5). A key consideration in the use of binders is their hydration process, as accelerating early-age hydration is essential for decoupling productive strength from service strength, thus improving its sustainability. This is particularly critical in printcrete, where the absence of formwork and the complexity of geometric shapes demand rapid strength development to ensure the structural performance of printed layers. In this paper, we primarily discuss systems developed by the authors in the context of hydration control, specifically those involving Portland cement, (sulfo) aluminate cement, and alkali-activated cement. While other materials, such as phosphate cement, limestone calcined clay cement (LC_3), and earth-based binders, also show potential for similar applications, will not be further discussed. Additionally, incorporating industrial by-products like mechanically treated garbage bottom ash and treated sugarcane bagasse ash can significantly enhance sustainability. However, as these materials have a limited effect on the hydration control of printcrete, this paper will not discuss them in detail. Further information can be found in Refs. [13,14].

2.2.1 Portland cement-based mixtures

Portland cement is the most widely used cement-based material in the construction industry due to its versatility and availability. However, it comes with certain drawbacks, such as low early-age strength and prolonged setting times, which are crucial for tunnel lining construction where rapid strength gain is required. This limits its applicability in printcrete.

To regulate these limitations, various chemical admixtures and mineral additives can be used to modify the performance of Portland cement. For instance, accelerators like aluminum sulfate are commonly added to enhance early-age strength [15]. Aluminum sulfate introduces additional aluminate ions into the mixture, which accelerates the hydration of tricalcium aluminate (C_3A), thus speeding up the early stages of hydration, as shown in Eq. (1).

$$2[Al(OH)_4]^- + 6Ca^{2+} + 4OH^- + 3SO_4^{2-} + 26H_2O \rightarrow 3CaO \cdot Al_2O_3 \cdot 3CaSO_4 \cdot 32H_2O \quad (1)$$

This process is particularly useful in applications such as shotcrete, where rapid setting is necessary to provide immediate support in excavations. Yet, it is important to note that the early-stage reaction primarily produces ettringite (AFt phase), releasing a significant amount of heat and being highly sensitive to temperature variations.

In the context of tunnel engineering, the construction environment can vary significantly, particularly in terms of temperature (a more prominent factor, especially for the high geothermal tunnels or in the case of using microwave curing) and pressure (a less critical factor). Changes in these environmental conditions can influence the hydration kinetics of cement, altering the overall behavior of the material during construction. To account for such environmental impacts on hydration, Pang et al. [16] have proposed a scale factor model to describe the effect of curing conditions on cement hydration, where the degree of hydration α can be expressed in Eq. (2):

$$\alpha = \alpha_{T,P}(t) = \alpha_{T_r,P_r}(Ct), \tag{2}$$

where α is the degree of hydration, T and P are the temperature and pressure of an arbitrary curing condition, T_r and P_r are the reference temperature and pressure, and C is the scale factor, which can be expressed as:

$$C_{T_r-T,P_r-P} = \exp\left(\frac{E_a}{R}\left(\frac{1}{T_r}-\frac{1}{T}\right)+\frac{\Delta V^{\ddagger}}{R}\left(\frac{P_r}{T}-\frac{P}{T}\right)\right), \tag{3}$$

where E_a is the apparent activation energy, $\Delta V^{\ddagger}$ is the apparent activation volume, R is the universal gas constant.

Previous studies have shown that the impact of the scale factor is minimal for tests conducted at different curing pressures, ranging from 0.7 to 51.7 MPa [16]. This suggests that pressure has a limited effect on the hydration kinetics of cement, thus supporting the notion that, in most cases, pressure can be disregarded when applying the scale factor model. It is important to highlight that the scale factor model represents constant external conditions, assuming constant external temperature and pressure throughout hydration, whereas in tunnel printing the material experiences dynamically changing external conditions during pumping and after extrusion (see more details in Subsection 3.1), factors that are absent in existing studies but are essential for accurately controlling hydration and achieving the desired material performance in practice.

2.2.2 Aluminate cement-based mixtures

Aluminate cements are available in several types, with calcium sulfoaluminate (C$A) cement and calcium aluminate cement (CAC) being the most used, where $ denotes the sulfate phase [8]. The first type to be discussed is the C$A cement, which is primarily composed of sulfate and aluminate phases. The primary hydration products are ettringite or monosulfate, along with amorphous alumina hydroxide, depending on the molar ratio of calcium sulfate to ye'elimite. A representative reaction is shown in Eq. (4).

$$C_4A_3\$ + 2C\$H_2 + 34H \rightarrow C_6A\$_3H_{32} + 2AH_3 \tag{4}$$

High sulfate levels in C$A cement can accelerate early hydration but may delay hydration at later stages. This can be managed using retarders, such as borax, which slow the hydration process [17]. The hydration can then be reactivated by adding a small amount of an alkali [18]. For instance, previous studies by Tao et al. [19,20] have utilized the ability of borax to initially retard C$A cement hydration and then reinitiate it with calcium hydroxide. This approach allows for better control over the open time of printcrete.

Due to the high cost of alumina-rich raw materials, C$A cement is often blended with other materials, such as Portland cement, to reduce costs. These blends are especially useful in two-component systems [20], where C$A cement provides early strength through the formation of ettringite, while Portland cement contributes to later-stage strength through the formation of C-S-H. Tao et al. [18] have studied the hydration mechanisms of these blended systems, where C$A cement and Portland cement are mixed in different ratios to control the hydration process in printcrete. The results indicate that maintaining a specific ratio is crucial for fine-tuning the hydration rate and achieving optimal performance.

The second alternative is CAC. CAC shares a similar hydration mechanism with C$A cement but relies on an external sulfate source, unlike C$A cement, which contains sulfate within its composition. Typically, CAC is mixed with gypsum, hemihydrate, or anhydrite. More details about CAC-C$ systems can be found in Ref. [21].

2.2.3 Alkali-activated mixtures

Alkali-activated cement could be used for printcrete. It is cost-effective due to readily available industrial waste, which reduces material costs and supports recycling efforts. Additionally, its production process requires less energy and results in lower carbon emissions than traditional Portland cement because it does not involve high-temperature calcination.

Several previous studies have explored the reaction mechanisms of alkali-activated materials (AAMs) with various precursors and activators, yet our focus here is on reaction control tailored for printcrete applications. Within the framework of a two-component strategy, Tao et al. [22] proposed a mixture design for AAMs specifically for this purpose. Their approach involves formulating two distinct streams: one based on slag

(without alkali content) and another on limestone powder (with varying alkali contents). These mixtures are designed to have indefinite open times, allowing for flexible handling. Once the two streams are merged before extrusion, the alkali activator in the limestone-based mixture immediately reacts with the slag precursor, triggering a rapid phase transition and setting process.

Building upon this technical approach, Sun et al. [23] developed a similar two-stream system using different precursors, including ground granulated blast furnace slag, which is highly reactive, and electric arc furnace slag, which has lower reactivity. By dividing the solid and liquid components of AAMs into two separate streams and intermixing them just before extrusion, a balance between workability retention during the pumping phase and accelerated reactions after extrusion can be achieved. A key advantage of this system is that both streams contain reactive precursors, unlike methods using inert limestone powder for the activator, which can lead to strength reductions in the final hardened material.

3 Required performance of printcrete

Concrete workability traditionally refers to the ease with which freshly mixed concrete can be placed, consolidated, and finished while maintaining homogeneity and preventing segregation. This concept has been fundamental to concrete technology for decades, as it directly affects the quality and durability of the final structure. With the development of printcrete, which involves multiple processing stages beyond traditional casting, the concept of workability has further diversified to address these unique challenges, including pumpability, extrudability, and buildability from the material's viewpoint. In addition to these terms, structural ability should be highlighted. Note that durability remains a vital consideration in the development and application of printcrete [24], while the detailed discussion of durability is beyond the scope of this paper.

3.1 Pumpability

Pumping is a widely adopted method in the modern concrete industry. In the context of printcrete, pumpability refers to the ability of concrete to be smoothly delivered from the mixing unit to the extrusion nozzle without experiencing any changes in its consistency while maintaining an acceptable level of pressure loss during pumping. A massive quantity of concrete is required to be pumped in a short time to form support structures such as tunnel linings.

In practical situations of long tunnels, achieving optimal pumpability for printcrete is particularly difficult if pumping over long distances. As the pumping distance increases, higher pressure is needed, leading to greater energy consumption and a higher risk of material segregation [25]. In tunnel engineering, this challenge is compounded by high-geothermal conditions. During long-distance pumping, elevated temperatures can accelerate early-age hydration, even though high pressure itself would have less effect on the reaction.

From a fundamental perspective, the flow behavior of fresh concrete, often treated as a non-Newtonian fluid, can be described using the Navier-Stokes equations:

$$\frac{\partial \boldsymbol{U}}{\partial t}+(\boldsymbol{U}\cdot\nabla)\boldsymbol{U}=-\frac{1}{\rho}\nabla p+\nu\nabla^2\boldsymbol{U}+(\nabla\boldsymbol{U}\cdot\nabla\nu)+\boldsymbol{f}, \tag{5}$$

where $\boldsymbol{U}$ is the velocity field vector, ρ is the fluid density (constant for incompressible flow), p is the pressure, $\boldsymbol{f}$ is the body force (e.g., gravity), ν is the kinematic viscosity ($\nu=\mu/\rho$), μ is the apparent viscosity of the material. In the equation, $\nu\nabla^2\boldsymbol{U}$ is the standard viscous diffusion term and $(\nabla\boldsymbol{U}\cdot\nabla\nu)$ is the additional term accounting for spatial gradients of viscosity. Since fresh concrete can be reasonably assumed to behave as an incompressible fluid at the scale of interest, the continuity equation simplifies to $(\nabla\cdot\boldsymbol{U}=0)$. Note that the kinematic viscosity ν is a critical parameter directly linked to both the chemical evolution of the material and its response to mechanical forces.

In practical printing scenarios, especially in tunnel applications where temperature variations can be significant during both pumping and after extrusion, both the intrinsic properties of the base mixture and the action of admixtures make viscosity strongly temperature-dependent, as these temperature fluctuations can significantly influence flocculation, dispersion, and the rate of structure build-up or breakdown in the material.

Another essential factor influencing viscosity is the shear rate $\dot{\boldsymbol{\gamma}}$, as fresh concrete demonstrates shear-dependent rheological properties, such as thixotropy and shear thinning. In the case of printcrete, the viscosity during shear can be more comprehensively expressed as:

$$\nu=\nu(\alpha,\dot{\boldsymbol{\gamma}},T), \tag{6}$$

where the shear rate $\dot{\boldsymbol{\gamma}}$ equals to $\left[\nabla\boldsymbol{U}+(\nabla\boldsymbol{U})^{\mathrm{T}}\right]$, and T is the temperature.

As rapid hydration reactions release substantial heat, significantly impacting the material's rheological behavior, the energy equation must be considered for printcrete:

$$\rho c_{\mathrm{p}}\left(\frac{\partial T}{\partial t}+\boldsymbol{U}\cdot\nabla T\right)=\nabla\cdot(k\nabla T)+\Phi+Q, \tag{7}$$

where c_{p} is the specific heat capacity, k is the thermal conductivity, Φ is the dissipation function, representing viscous heating, and Q is the heat generation rate from

hydration, which relates to the rate of hydration and the temperature:

$$Q = Q(\alpha, T). \tag{8}$$

Therefore, monitoring temperature during mixing and pumping would help to master the degree of hydration, as well as the estimation of rheological properties.

3.2 Extrudability

Extrudability of printcrete refers to the capability of the material to be pushed through a nozzle in a continuous, uniform filament. This characteristic is essential to ensure that the concrete flows smoothly during the printing process and enables the following formation of stable and cohesive layers that contribute to the overall structural integrity. That is, there are two aspects to ensure extrudability: no clogging at the nozzle and sufficient cohesion of the extruded filament.

Clogging can occur even when the nozzle diameter is identical to that of the pumping pipe. Fundamentally, clogging is influenced by several factors, including the friction between aggregates since higher content or/and larger size, the interaction of the particles within the mixture, and the increase of viscosity with hydration. For maintaining a smooth extrusion process, monitoring pressure at the extrusion nozzle might help in avoiding clogging. Tao et al. [26] made use of computational fluid dynamics (CFD) to simulate the extrusion process and evaluate the geometrical profiles of printcrete. The cross-sectional geometry of the virtual prints shows a qualitative agreement with the physical prints, indicating that the simulation closely replicates the actual printing process, as shown in Fig. 3.

The other index on extrudability is the ability of the filament to achieve sufficient cohesion. Printcrete is relatively stiff and behaves more like a jammed, concentrated suspension. In physics, such materials exhibit shear localization, where shear deformation is confined to a narrow region whose thickness decreases with increasing solid fraction. At high solid fractions and strong particle interactions, this localization can lead to cracking behavior like that observed in brittle solids. To mitigate the risk of cracking during extrusion, the tensile strength or critical strain of the fresh printable material can be increased.

3.3 Buildability

Buildability describes the ability of the extruded concrete to retain its shape and support subsequent layers without collapsing or deforming, before hardening. This characteristic is essential to ensure the stability and integrity of the printed structure throughout the construction process. Two types of failures related to buildability have been pointed out: elastic buckling and plastic collapse [27]. Elastic buckling is associated with the elastic modulus of the material, while plastic collapse relates to the static yield stress, or green strength. That is, static yield stress is particularly relevant after the material has been extruded and deposited, as it determines the ability of the freshly printed layers to support subsequent layers without collapse. More recently, research has also explored the combined effects of these two failure modes on the stability of printed concrete structures [5].

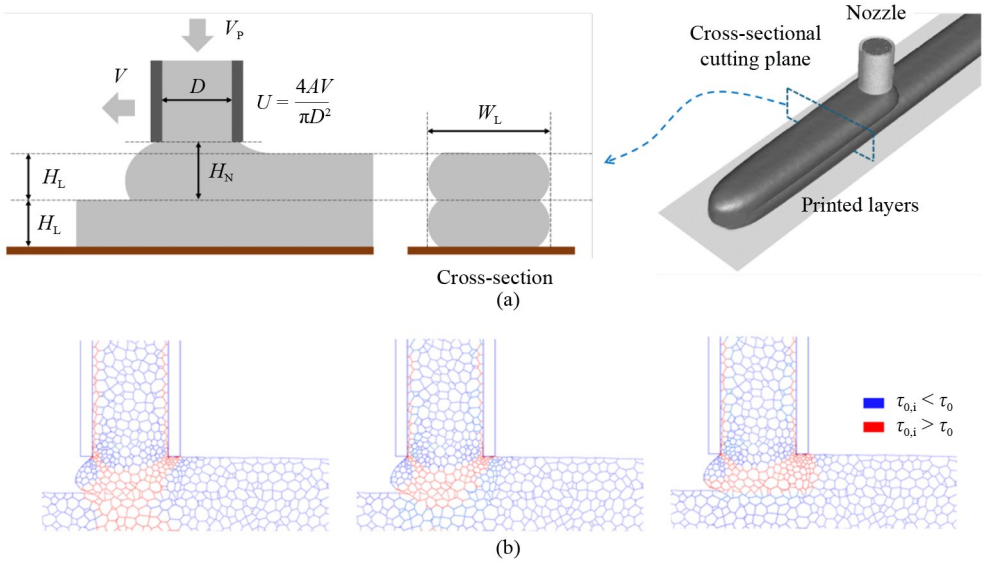


Fig. 3 CFD model for buildability evaluation: (a) a schematic representation of the extrusion configuration with two layers is presented, and (b) distribution of plastic yielded region, which is indicated in red color. The figure is adapted from Ref. [26] (Reprinted from Materials and Structures, 57, Tao Y, Zhou J, Cui W, Shi X, de Schutter G, van Tittelboom K, Numerical assessment of plastic yielding in extrusion-based 3D concrete printing, 65, Copyright 2024, with permission from Springer Nature).

For printcrete applications in tunneling engineering, the requirements for buildability differ slightly from those in above-ground structures. As printcrete is extruded against the excavated surface of the surrounding rock, the material needs to adhere effectively and firmly onto the surface and, subsequently, gain strength rapidly to prevent possible failures (Fig. 4). The extruded material as tunnel linings must not only support itself and subsequent layers but also require developing sufficient strength quickly to support the loose rock, and stiffness to confine the convergence of the tunnel configuration.

Achieving sufficient interfacial adhesion between printcrete and rock is a complicated process. Tests conducted by Tao et al. [29] have shown that air voids would form at the interface, particularly when using materials with a high yield stress that are more challenging to deform and ensure full contact with the rock. A rough rock surface can exacerbate this issue. Although increasing the moisture content or adding cellulose ether can improve the fresh stage adhesion of printcrete [30], the maximum adhesion force achieved to date is only sufficient to support a tunnel lining thickness of around 100 mm at the crown position [31]. Higher lateral adhesion values can be achieved for the side wall positions. Nonetheless, effective technologies to enhance interfacial adhesion are still lacking. Moreover, a key limitation is the lack of quantitative methods to accurately assess the properties of the substrate, especially the moisture content of the substrate, which are crucial for optimizing adhesion. These quantitative approaches need to be developed and extended to further improve the understanding and effectiveness of the bonding process at the interface.

The shape stability of a printed layer can vary widely depending on the specific mixture design and the design target. For instance, the thickness of printed layers can range from as little as 1 mm for paste filaments to as much as 100 mm for concrete deposition [32]. Thicker filaments are more susceptible to shear forces induced by gravity, which can impact their stability. Therefore, in situations requiring significant structural build-up, it is essential to consider both the setting time and early-age strength of the printcrete, as in shotcrete.

Another essential method to accelerate early-age strength development is through manipulating the external environment, primarily by employing curing techniques. The curing methods aim to balance early acceleration with maintaining or even improving the later-age strength of printcrete. Further details about the specific curing devices and strategies are covered in Subsection 5.4.

3.4 Structural ability

Structural ability of printcrete describes the overall performance and stability of a completed printed element or structure. This includes considerations such as structural load-bearing capacity and the ability to withstand various environmental and operational actions.

The structural performance of printcrete for tunneling engineering, particularly regarding the entire structure and its service life, is of significant interest. Bearing capacity under loads, fire resistance, durability under environmental actions, and dynamic resilience during seismic and impact, of printcrete with or without reinforcing bars, are some of the indices to account for its structural ability. Evaluating the response of lining structures to earthquakes is essential for understanding their behavior under real-world conditions [33,34]. To provide valuable insights into how well the printed layers bond under dynamic conditions, how energy is dissipated across the structure, and how potential weaknesses can be mitigated, techniques such as the shaking table test are critical.

The fire resistance of printcrete is another critical consideration, particularly for tunneling engineering, where fire safety is paramount. Fire resistance involves assessing the ability of printcrete to withstand high temperatures without significant loss of structural integrity [35,36]. The thermal conductivity, heat resistance, and potential spalling behavior of printcrete must be thoroughly evaluated.

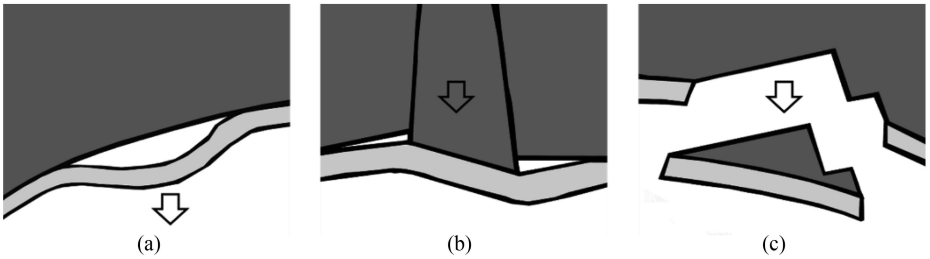


Fig. 4 Typical failure of tunnel linings: (a) adhesion failure; (b) adhesion failure due to punching; (c) shear failure due to punching. Dark grey indicates excavated rock, and light grey indicates tunnel lining. The figure is adapted from Ref. [28] (Reprinted from Cement and Concrete Composites, 131, Tao Y, Lesage K, van Tittelboom K, Yuan Y, de Schutter G, Influence of aluminum sulfate on mobility and adhesion of hydroxyethyl methyl cellulose in cement-based materials for tunnel linings, 104594, Copyright 2022, with permission from Elsevier).

In general, key boundary conditions such as mechanical forces and temperature must be rigorously assessed to ensure the structural integrity of printed tunnel structures. Moreover, the interaction between mechanical forces and temperature, as well as the moisture content discussed in Subsection 3.3, needs to be evaluated in a coupled manner. The simultaneous effects of these factors are likely to create complex stress states within the printed structure, which could influence the structural ability. Future studies should focus on developing models that integrate these boundary conditions, enabling a more comprehensive understanding of their combined effects on printed tunnel structures.

4 Characterization of printcrete

Printcrete represents a transit process from a particle material to a solid structure, undergoing many stages that should be characterized with indices and be evaluated with proper approaches. This study focuses on the most critical stages within the process.

4.1 Rheological properties

For fresh cementitious materials, rheological parameters can be used to represent flowability during mixing and pumping, but after extrusion of printcrete. However, after the extrusion of printcrete, its rheological characteristics continue to evolve. As previously mentioned, the flow behavior of such materials is non-Newtonian and varies not only with shear stress, but also due to ongoing hydration, temperature changes, and other influencing factors. This sub-section focuses specifically on the yield stress and viscosity characteristics of printcrete.

4.1.1 Yield stress

Conventional test methods such as the slump test, slump flow test, and L-box test, and are commonly employed to evaluate the flowability of fresh concrete. Based on empirical correlations and measurement-derived equations, slump values can be converted into estimates of yield stress. Although slump has been used as an index for designing printable concrete, it does not provide an accurate characterization of the yield stress specific to printcrete. In contrast, a rotational rheometer equipped with a container and a coaxial vane (or spindle) offers a more advanced and reliable approach for measuring the yield stress of cement-based materials. It can directly determine either the static or dynamic yield stress; however, it is not suitable for real-time (in-line) measurements during the printing process.

In addition to conventional testing methods and rotational rheological measurements, several specially designed approaches have been developed specifically for printcrete. One notable example is the squeeze flow test [37], which has been well-developed and has recently been applied to the characterization of printcrete by Tao et al. [11], as illustrated in Fig. 5. This test involves placing a fresh printcrete sample between two parallel plates and applying a compressive load to measure the material's deformation behavior under stress. The test setup allows for the simultaneous measurement of yield stress using constant force squeeze flow, where the so-called modified yield stress $\tau_{0,\mathrm{m}}$ considering the correction factor is expressed as:

$$\tau_{0,\mathrm{m}} = \frac{3Fh_{\mathrm{L}}}{2\pi F_{\mathrm{AR}} R^3}, \tag{9}$$

where F is the compression force, h_{L} is the gap between two plates at the steady state, F_{AR} is the correction factor, and R is the radius of the plates.

In the author's viewpoint, the yield stress is a time-dependent behavior of printcrete after mixing, during pumping, and before extrusion. It is better to develop an inline measuring method to get its on-time value.

4.1.2 Viscosity

In this section, we focus primarily on the viscosity of printcrete during the pumping process, where the material is subjected to shear stress, and its flow characteristics are governed by the flow rate or shear rate. However, in other stages, such as deposition, viscosity is less critical since the material is no longer under significant shear stress, and other properties like buildability and early strength gain become more important.

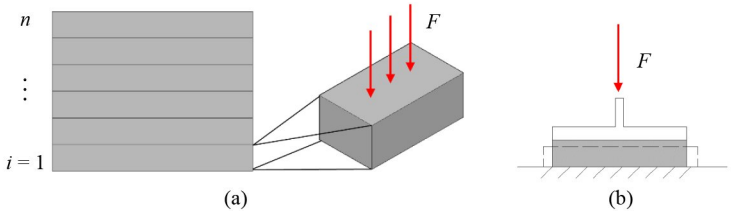


Fig. 5 Illustration of the squeeze flow test: (a) 3D printed layer configuration; (b) deformation of printcrete under compression. The figure is sourced from Ref. [11] (Reprinted from Cement and Concrete Composites, 133, Tao Y, Ren Q, Lesage K, van Tittelboom K, Yuan Y, de Schutter G, Shape stability of 3D printable concrete with river and manufactured sand characterized by squeeze flow, 104674, Copyright 2022, with permission from Elsevier).

Conventionally, viscosity is evaluated using parameters obtained from standardized tests such as the T500 slump flow test and the V-funnel test. In these tests, the flow of the material is observed, and the time it takes to reach a specific position is recorded, from which a viscosity value can be indirectly calculated. While these tests are relatively simple to perform, the viscosity values they produce are not highly accurate or straightforward, which may not suffice for the precise rheological control needed in printcrete.

Flow curves can yield precise results by measuring the material's response to different shear rates [8,38]. However, practical challenges arise due to the limitations of the torque that can be applied by the rheometer. In scenarios involving stiff materials like printcrete, the torque capacity of the instrument can be easily exceeded, restricting the range of measurements that can be performed. Although reducing the size of the measuring geometry, such as the blades or spindle, offers a partial solution to this issue [39], this approach still faces practical limitations such as loading the testing geometry into the stiff printcrete material and ensuring that the results are representative of the material's behavior under actual pumping conditions.

Beyond experimental approaches, a mathematical model for the apparent viscosity of fresh cement-based materials has been proposed by Yuan et al. [40]. This model considers various factors, such as the water-to-cement ratio and the addition of superplasticizers (Eqs. (10) and (11), respectively), which significantly influence the viscosity of cement-based materials. The model is derived from the Navier-Stokes equations and the Ostwald model. By incorporating additional parameters, such as the degree of hydration and the presence of aggregates, the model can become highly efficient for predicting the rheological behavior of printcrete. This predictive capability is particularly useful for optimizing mixture designs and ensuring the material's pumpability in practical applications.

$$\eta = \left[D_1(w/c)^{D_2} + D_3\right]\dot{\gamma}^{C_1 w/c-1}, \tag{10}$$

where η is the viscosity of the whole domain in an arbitrarily known y position, w/c is the water-to-cement ratio, $\dot{\gamma}$ is the shear rate, D_1, D_2, D_3, and C_1 are calculation parameters.

$$\eta \approx F_1(n_S)\left[d_1(w/b)^{D_2} + d_3\right]\dot{\gamma}^{F_2(w/b,n_S)w/b-1} + F_3(w/b,n_S), \tag{11}$$

where n_S is the dosage of superplasticizer, w/b is the water-to-binder ratio, d_1 and d_3 are calculation parameters. The detailed expression of F_1, F_2, and F_3 can be found in Ref. [40].

4.2 Structural build-up

Structural build-up of printcrete, just as cement-based materials, primarily arises from two sources: thixotropy due to flocculation (a reversible process) and hydration (an irreversible process) [41]. Flocculation involves the formation and breakage of colloidal interactions and C-S-H nucleation at the contact points between cement particles within the paste, which can be reversed under shear. In contrast, hydration is a chemical process involving the reaction of cement with water, leading to the formation of hydration products that contribute to the progressive stiffening and hardening of the material. Given the emphasis on rapid strength gain and buildability in printing applications, understanding the structural build-up due to hydration is especially crucial.

To experimentally quantify the structural build-up of cementitious materials, rheological and non-rheological techniques were proposed. One effective method is the small amplitude oscillatory shear (SAOS) test, which monitors the evolution of the material's structure at rest [42]. SAOS has proven effective for testing cement pastes, particularly when a rheometer with high precision is used. However, this method becomes less suitable for printcrete, which typically contains aggregates. The inclusion of aggregates complicates the measurement process, as the very small amplitude oscillations required for accurate SAOS measurements are not feasible with coarser, heterogeneous materials like printcrete.

A more efficient method is the slow penetration test, which provides a continuous measure of yield stress evolution. This test involves slowly penetrating a rod or a probe into the material at a controlled rate, allowing the resistance force encountered to be measured continuously. The slow penetration method offers several advantages, including its ability to monitor changes in yield stress over time without the need for multiple separate measurements. Tao et al. [43] have employed the slow penetration test to monitor the yield stress evolution of printcrete, see yield stress evolution in Fig. 6(b), demonstrating its potential for providing real-time data on buildability during the printing process. An alternative approach for assessing structural build-up in printcrete involves using ultrasonic pulse velocity (UPV) testing [44]. This method measures ultrasonic wave speed passing through the material, which can be correlated with changes in density and stiffness as hydration progresses, see P-wave velocity curves over time in Fig. 6(a). While UPV testing has been widely used to correlate wave velocity with compressive strength development [45], it does not directly relate to the yield stress of the material, which is more critical for determining buildability in printcrete applications.

Similar trends were observed in both the UPV and slow penetration tests, where the yield stress of mixture A-B2

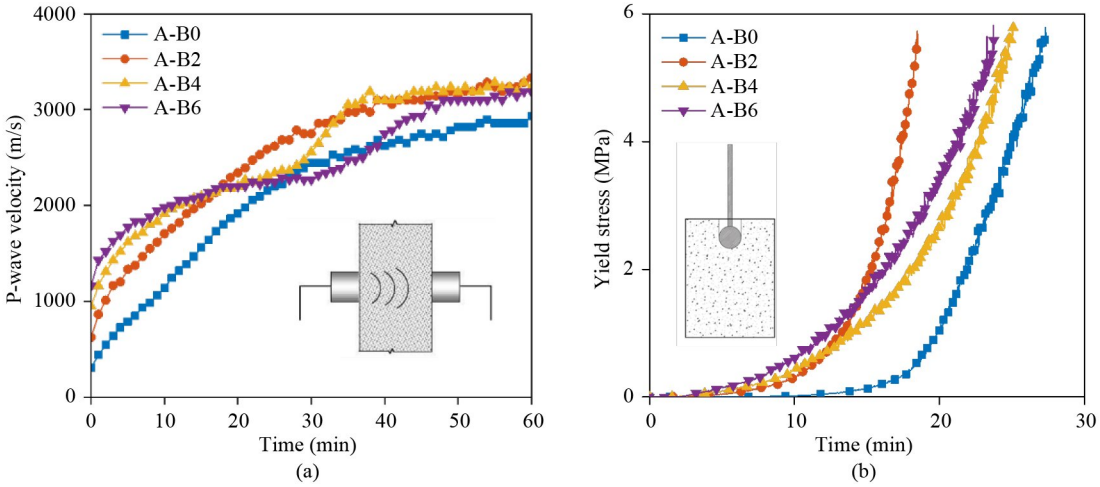


Fig. 6 Structural build-up of printcrete: (a) P-wave velocity from UPV tests; (b) yield stress from slow penetration tests. Mixture A: retarded CSA cement-based; Mixture B: Portland cement with 0%–6% $Ca(OH)_2$ replacement. Both were mixed at equal volume before testing. The figure originates from Ref. [20] (Reprinted from Cement and Concrete Composites, 138, Tao Y, Mohan M K, Rahul A V, de Schutter G, van Tittelboom K, Development of a calcium sulfoaluminate-Portland cement binary system for twin-pipe 3D concrete printing, 104960, Copyright 2023, with permission from Elsevier).

was initially lower than that of mixtures A-B4 and A-B6 during the first 15 min (see the mixture design of A-B in Ref. [20]). However, after this period, the yield stress of A-B2 surpassed the other two mixtures. This same behavior was reflected in the P-wave velocity evolution. While these findings offer valuable qualitative insights into the performance of the mixtures, further investigation is needed to establish a quantitative correlation between the different testing methods.

4.3 Interfacial adhesion

As discussed in Section 3 regarding the performance requirements of printcrete, interfacial adhesion plays a critical role in ensuring both buildability and structural ability. In this section, we concentrate on the characterization of the interfacial adhesion of printcrete in its fresh state. While numerous methods have been developed and are well-established for evaluating the adhesion, or bond strength, of repair materials in their hardened state [46], the evaluation of adhesion in the fresh state remains relatively unexplored.

A tack test developed by Tao et al. provides a quantitative method for evaluating the interfacial adhesion performance of printcrete, particularly focusing on the detaching failure mode, where failure occurs at the interface (Fig. 7) [19,28,29,31]. This method utilizes two parallel plates to simulate the adhesion process. In the test setup, a fresh sample of printcrete is placed on the bottom plate. The top plate is then moved downward to a specific gap (usually equal to the thickness of a single printed layer) to establish contact between the fresh sample and the top plate. To accurately mimic the properties of the substrate, a drilled rock or concrete specimen can be attached to the top plate to replicate the surface of an excavated wall. After the initial contact, the top plate is lifted in either a load-controlled or displacement-controlled mode, following a protocol like a 3D printing process. Throughout this procedure, tensile force versus displacement curves is recorded. Key indices such as maximum tensile force, critical displacement corresponding to the maximum tensile force, and the energy required for detaching the two plates are used to evaluate interfacial adhesion. This approach allows for the investigation of various factors affecting adhesion, such as different levels of substrate roughness and moisture content, by pre-treating the drilled rock or concrete substrate.

In addition to the tack test, a modified pull-out test for fresh materials has also been proposed by Tao et al. [19]. This test is adapted from the traditional bond test used for hardened concrete, where a steel plate is placed at the interface before the concrete is cast. Similar to the tack test, the steel plate is then lifted, and the tensile force versus displacement is recorded. One of the main advantages of this method is its ability to simulate the punching failure process, which helps in understanding whether the failure occurs at the interface or within the material itself.

In addition to adhesion in the normal direction, the adhesion of printcrete in the shear direction with rock has been investigated by Yuan et al. [47], particularly focusing on the super early age of printcrete. An innovative testing method involving a push-shear test of cylindrical samples was developed for this purpose (Fig. 8). The results, presented in a dimensionless format, provided valuable insights into how various factors, such as surface roughness, aggregate size, and the strength grade of the printcrete, affect shear adhesion, as described using the following equation:

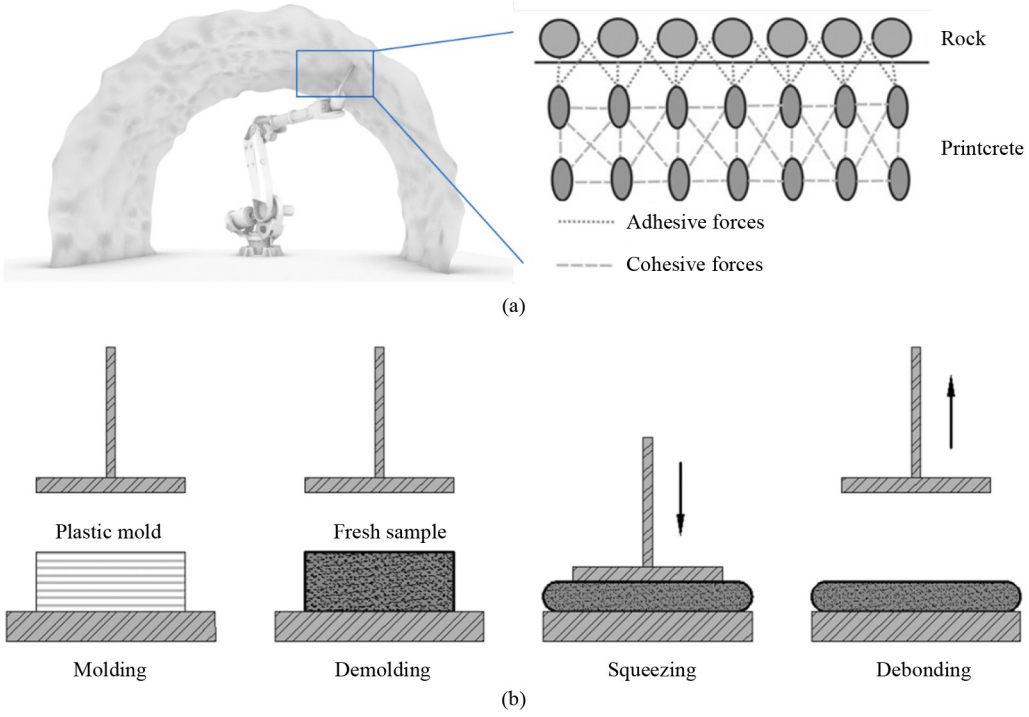


Fig. 7 Adhesion evaluation of printcrete: (a) schematic of adhesive and cohesive force; (b) procedure of the tack test, including molding, demolding, squeezing, and debonding. The figure is adapted from Refs. [29,31] (Reprinted from Cement and Concrete Composites, 126, Tao Y, Lesage K, van Tittelboom K, Yuan Y, de Schutter G, Influence of substrate surface roughness and moisture content on tensile adhesion performance of 3D printable concrete, 104350, Copyright 2022, with permission from Elsevier; Reprinted from Automation in Construction, 149, Tao Y, Ren Q, Vantyghem G, Lesage K, van Tittelboom K, Yuan Y, de Corte W, de Schutter G, Extending 3D concrete printing to hard rock tunnel linings: Adhesion of fresh cementitious materials for different surface inclination, 104787, Copyright 2023, with permission from Elsevier).

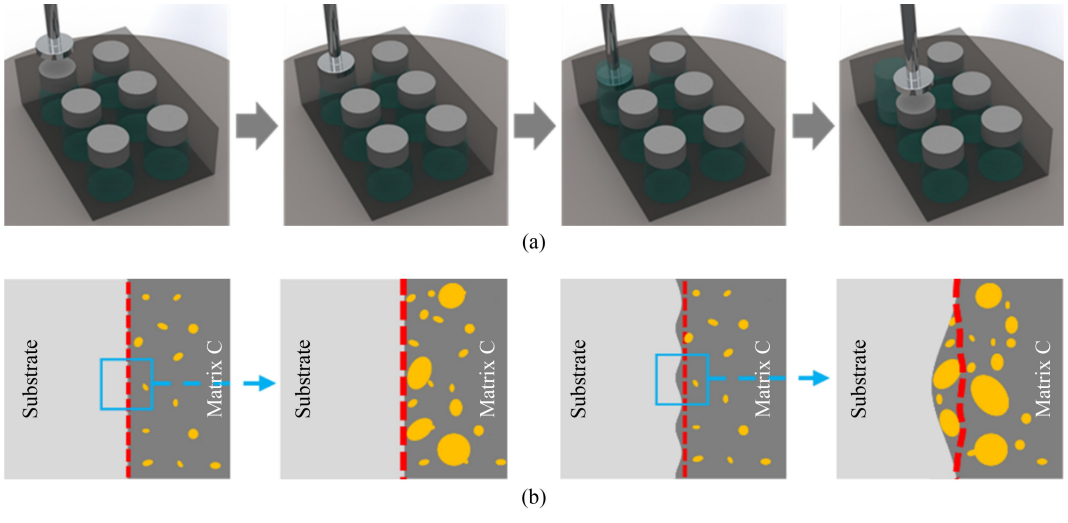


Fig. 8 Push-shear test: (top) the testing procedure, including aligning the axes, moving down the loading rod toward the sample, loading until debonding, and testing for the next sample, (bottom) schematic of failures with low and high roughness levels. The figure is adapted from Ref. [47] (Reprinted from Frontiers of Structural and Civil Engineering, 18, Yuan Y, Wang X, Zhang J L, Tao Y, van Tittelboom K, Taerwe L, de Schutter G, The shear strength of the interface between artificial rock and printed concrete at super-early ages, 51–65, Copyright 2024, with permission from Springer Nature).

$$\frac{\tau}{\tau_0}=\left(\frac{t'}{\Delta t}+1\right)^{a}\cdot\left(1\cdot\frac{1}{1+c\cdot\dfrac{Z_1Z_2}{D_{50}}}+b\cdot\frac{c\cdot\dfrac{Z_1Z_2}{D_{50}}}{1+c\cdot\dfrac{Z_1Z_2}{D_{50}}}\right), \quad (12)$$

where τ is the shear strength, τ_0 is the shear strength at the age of the 1st minute after the final setting, a represents the time-dependent rate of matrix increment, b denotes the ratio between bulk material shear strength and

interface shear strength, c relates to the transition between failure modes, Z_1 and Z_2 are used to quantify the effect of interface roughness, D_{50} is the mean particle size of aggregates, t' is the age after the final setting, and Δt is the time gap between the initial and final setting.

5 Equipment for printcrete

Printcrete requires specialized equipment to ensure the precise and efficient delivery of concrete materials. The basic components of a printcrete system typically include a mixer, a pump, a printing head (or nozzle), and, in some cases, a curing device. Each of these components plays a crucial role in the process, from mixing raw materials to extruding the concrete into the desired shape and finally ensuring the material's early strength and durability. In this section, we provide an overview of the current devices used in printcrete technology and explore potential advancements in these systems, especially considering the growing trend toward intelligent construction.

5.1 Smart mixers

The mixer is the first critical component in the printcrete process. While traditional batch mixers can still be used, future advancements will require the development of smart mixers capable of real-time adjustments to the mixture composition and mixing parameters based on feedback from monitoring systems. One innovative approach involves the use of image-capturing technology to assess the uniformity of the mixture [48,49]. Another method estimates the viscosity of fresh concrete using torque transducers [49]. Figure 9 presents the results of implementing such a smart mixer system.

However, several challenges remain. These include extracting key information from images to accurately assess mixture uniformity and continuously monitoring motor torque to determine precise rheological properties. In this context, artificial intelligence (AI)-assisted image processing can be employed to analyze surface features of the mixture. Furthermore, to anticipate the hydration process, continuous monitoring of the material's temperature is also necessary.

5.2 Sensor-based transport system

In practical applications, several types of pumps are commonly employed for transporting fresh concrete, including piston pumps, auger pumps, and peristaltic pumps [50], as shown in Fig. 10. Each type of pump has distinct advantages that influence its selection based on the specific requirements. Piston pumps are known for their ability to deliver high pumping pressures, reaching up to 130 bar [51], making them ideal for applications requiring substantial force to move the material. Moreover, the maximum aggregate size that a piston pump can

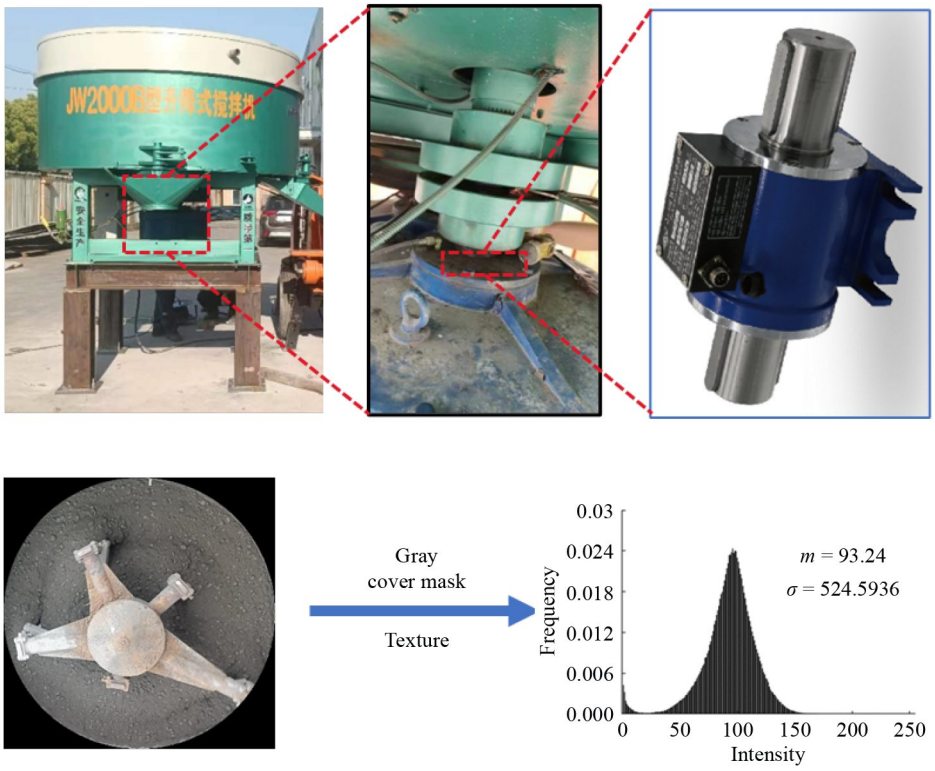
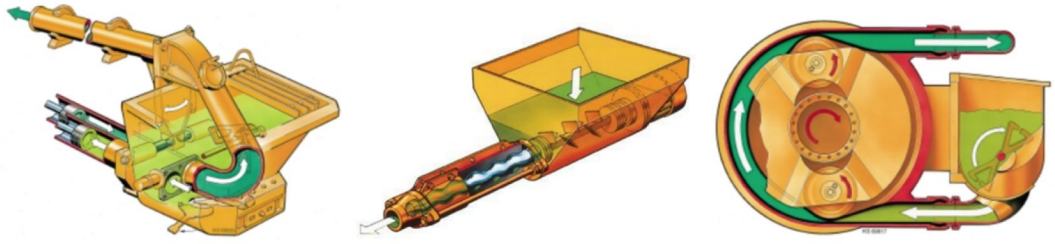


Fig. 9 Smart mixer system for printcrete, featuring a torque transducer and image analysis for real-time monitoring of rheological properties and mixture uniformity.



(a) (b) (c)

Fig. 10 Schematic view of concrete pumps: (a) piston pumps; (b) auger pumps; (c) peristaltic pumps.

deliver is up to 40 mm, making it suitable for all types of concrete mixtures [52]. However, they operate in a pulsating manner, creating pressure peaks and shock waves that can affect the uniformity of flow. Unfortunately, this nonuniformity is not ideal for printcrete, which requires a consistent flow rate to maintain proper layer morphology. In contrast, auger pumps and peristaltic pumps provide a more continuous flow, which is beneficial for maintaining a steady supply of the suspension without the fluctuations seen in piston pumps. While auger and peristaltic pumps offer a smoother flow, their maximum deliverable pressures are typically lower, generally below 40 bars [53]. In addition, the maximum aggregate size that can be delivered using an auger or peristaltic pump is relatively smaller, around 20 mm, due to the smaller chamber size compared to a piston pump. Nevertheless, the peristaltic pump offers the added benefit of having minimal maintenance requirements, as only the inner, flexible tubing needs regular cleaning and replacement due to wear.

Currently, most pumps used for printcrete are auger pumps. This is largely because most printcrete applications today involve mortar or concrete with relatively small coarse aggregates, allowing the auger pump to stay within the size limits while providing a consistent flow rate. However, for practical applications, there is a need to scale up the concrete mix and increase the aggregate size, as well as the flow rates. This, in turn, imposes additional requirements on the pumps and necessitates further research and development.

An effective method to monitor the pumping process involves the use of pressure, velocity, and thermal sensors. By placing multiple sensors along the length of the pipeline, the pressure loss over the entire pumping distance can be measured, and any significant deviation or sudden pressure drop can signal a potential blockage or build-up, minimizing the risk of pipe bursts and ensuring a smooth and continuous pumping process. In addition to pressure, monitoring the flow rate is another critical parameter, especially for printcrete, where a consistent and controlled flow is necessary for achieving the desired print quality. An electromagnetic flow rate meter can be used to measure the flow rate accurately [54]. However, this device requires calibration for each different mixture design, which limits its use as an independent measurement device.

To prevent total blockages and pipe bursts, it is also essential to detect fouling inside the pipe. One method that has been explored is using an ultrasonic velocity profiler (UVP) to capture the velocity profile of the material within the pipe [55]. Although this technique has shown some promise, the presence of coarse or even fine aggregates in the paste can introduce significant noise into the signal, affecting the accuracy of the velocity profile output. As a result, only the acoustic Doppler spectrum has been used for qualitative comparisons so far [56]. To date, no comprehensive studies have been conducted to quantitatively analyze the data captured by UVP for fouling detection in printcrete applications. Therefore, there is a significant opportunity for future research to explore this area in more detail, providing deeper insights into the general mechanisms of pipe fouling and potential strategies to mitigate it in printcrete applications.

5.3 Nozzles

5.3.1 X-component systems

To differentiate between various systems used in printcrete applications, we use the character “X” to denote one-component, two-component, or multiple-component systems [8]. The most used system is still the one-component system, primarily due to its simplicity and ease of operation. This system typically relies on the thixotropic properties of the material without any active control mechanisms right before extrusion. However, the one-component system has notable drawbacks, i.e., relying solely on the thixotropy of the material makes it difficult to achieve the necessary early-age strength needed for the effective support of loose rock in tunnels.

In contrast, the two-component system offers a more sophisticated approach. In this setup, two separate streams of material, each with high fluidity and an extended open time, are pumped separately to satisfy the pumpability requirements. These two streams then react with each other immediately before extrusion, accelerating the hydration process to meet the buildability needs

of tunnel structures. There are two main categories within the two-component systems: static mixing systems and dynamic mixing systems [57–59], as shown in Fig. 11. Static mixing systems, where the two streams are mixed passively as they pass through a static mixer, are advantageous because they do not require external power and are generally simpler to maintain. However, they may struggle with achieving uniform mixing homogeneity, especially if the materials have significantly different viscosities or flow properties. Dynamic mixing systems, on the other hand, utilize mechanical mixing elements or agitators, which provide better mixing homogeneity and can handle a wider range of material viscosities. However, they require external power to move the material through the system. A detailed comparison of these two systems has been systematically analyzed by Wangler et al. [8].

One novel approach within the two-component systems is the concept of twin-pipe pumping, which introduces a carrier material that contains an accelerator or other activators (see mixture design in Subsection 2.2) [20,22,43,60]. This method has several advantages, such as reducing the reaction rate at the inlet of the accelerator, thereby lowering the likelihood of blockages, and enhancing the efficiency of mixing by balancing the rheological properties of the two streams. By using a carrier material, the activator is more evenly distributed throughout the cement paste, leading to a more controlled hydration process and minimizing the risk of premature hardening that could block the reactor.

Currently, the most complex system in use is a three-component system, such as the one developed at ETH Zurich [8]. In this setup, an accelerator and a viscosity-modifying admixture are injected separately into the printing system. This approach allows for precise control over the mixture, with the viscosity-modifying admixture ensuring immediate shape stability for each layer and the accelerator enhancing later-age buildability. While this system provides a high degree of control, it also introduces additional challenges. Compatibility between flow rates and the potential increase in pumping pressure can complicate overall system management. Balancing these factors is crucial for achieving optimal performance in printcrete applications, particularly in demanding environments such as tunnel construction.

5.3.2 Control of inline mixing

For two-component systems (or multi-component systems) used in printcrete applications, it is crucial to continuously monitor the mixing homogeneity and detect any potential blockages within the mixing chamber, especially given the rapid reactions that occur inside. Real-time monitoring provides accurate information, which is essential for maintaining consistent mixing quality and enables the system to initiate automatic cleaning processes based on the feedback received.

In this context, image analysis presents a promising solution. For example, an in-line dye tracer strategy has been proposed to measure the residence time in continuous concrete processing [61], allowing for the monitoring of mixing efficiency in real-time. Similar tracer techniques have been utilized by Wangler et al. [8] to assess the mixing efficiency of in-line dynamic mixers. However, current technologies also have limitations. It is challenging to extract key information from images due to the complexity of visual data and the rapid dynamics within the mixing chamber. These challenges are similar to those encountered in smart mixers employing image recognition technologies.

Another significant challenge for two-component or multi-component systems is developing a self-cleaning function that integrates seamlessly into the overall process. This challenge is practical because all functions, including printing path control, pump regulation, the in-line mixing module (particularly in dynamic mixing

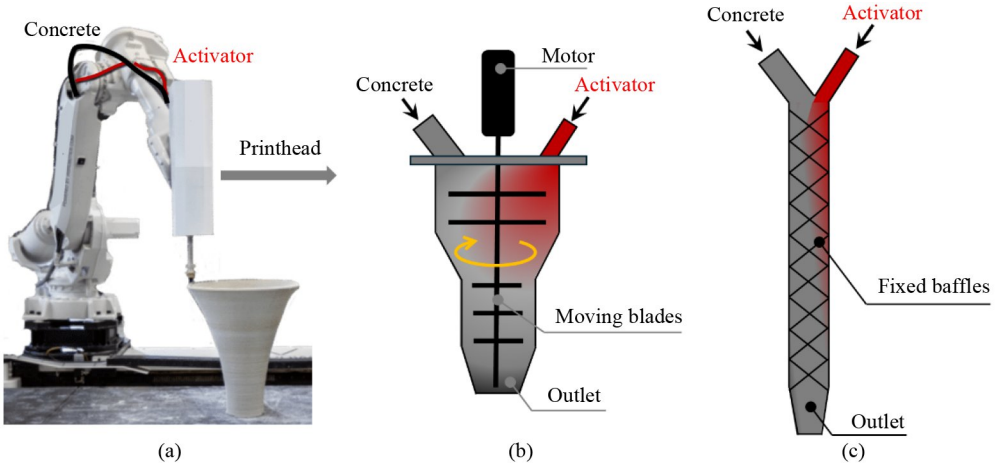


Fig. 11 Illustration of two-component systems: (a) general schematic of two-component printhead on a robot arm; (b) schematic of an active mixing system; (c) schematic of a static mixing system. The figure is sourced from Ref. [8].

systems), and the outlet of the material, must be synchronized. An integrated system is necessary to manage the complex coordination required for effective in-line mixing and self-cleaning. A protocol developed by the authors, as illustrated in Fig. 12, outlines different procedures for managing interruptions in the mixing process. Considering the fast reactions inside the in-line mixing chamber, different strategies must be employed depending on the duration of interruptions. For short interruptions, simply stopping the pumps and controlling the valves may suffice. However, if the interruption lasts longer than several seconds, the mixing chamber must be promptly flushed to avoid blockages.

To address the risk of blockages during longer interruptions, a low-reactivity stream can be introduced to flush the mixing chamber, thereby preventing rapid reactions from occurring. Following this, an automatic water valve can be employed to flush out any remaining low-reactivity material to ensure that no residuals remain that could cause a blockage. This multi-step procedure, designed to maintain the cleanliness and functionality of the mixing chamber, is crucial for the uninterrupted operation of printcrete systems and is detailed in Fig. 12.

5.4 Curing devices

Generally, curing methods can be classified into two main categories: external curing and internal curing. External curing involves methods such as steam curing, autoclave curing, oven curing, and microwave curing [62]. These methods have been extensively covered in the literature and are commonly used to enhance the strength and durability of concrete by providing an optimal environment for hydration. Internal curing (also known as self-curing), on the other hand, involves incorporating materials such as superabsorbent polymers, lightweight aggregates, or other internal curing agents into the concrete mixture [63]. This approach focuses on retaining moisture within the concrete itself, rather than relying on external devices or environmental control, and is more related to the mixture design of concrete rather than external application. However, this section focuses specifically on microwave curing, an advanced technique that has proven particularly effective in accelerating the hydration reaction of printcrete after extrusion, providing crucial early-age support for tunnel structures.

Microwave curing offers several advantages over

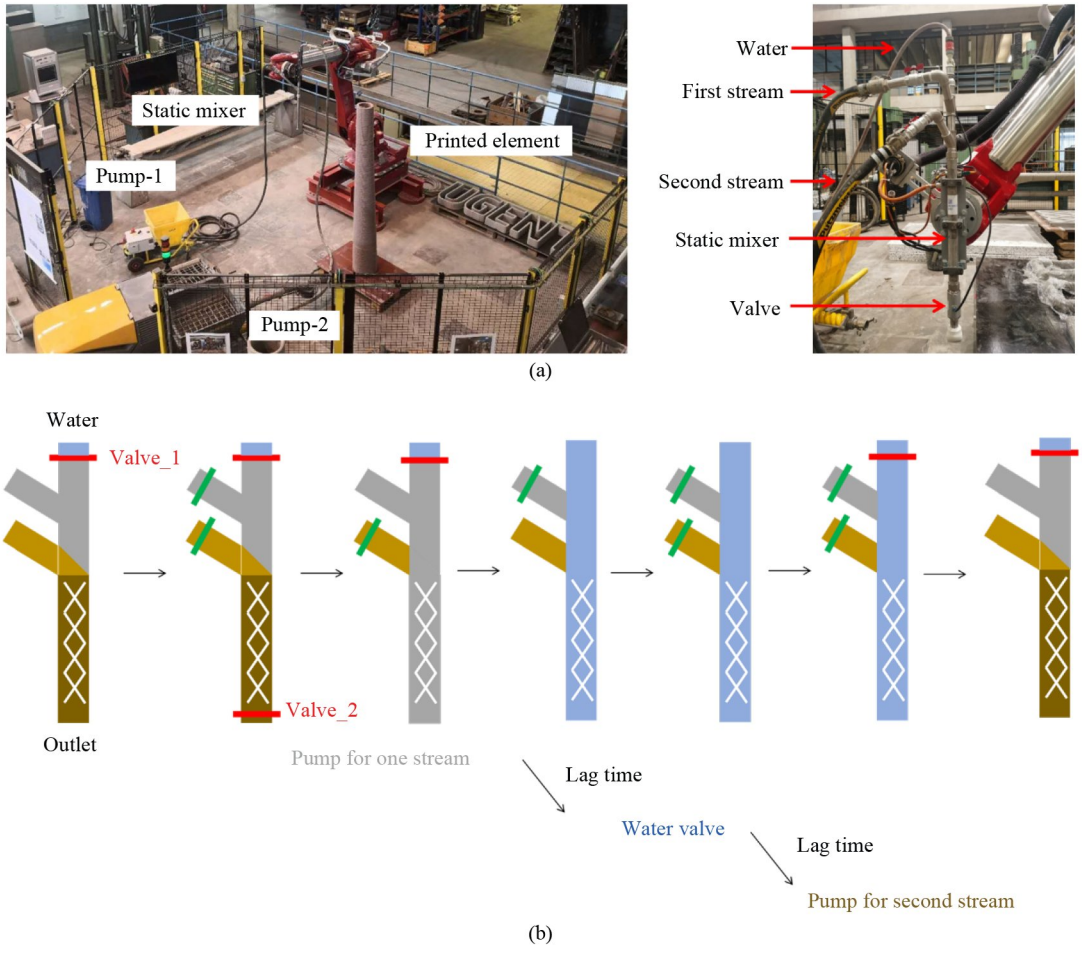


Fig. 12 Automatic cleaning function developed for the twin-pipe pumping system: (a) twin-pipe pumping and 3D printing nozzle equipped with a water pipe for cleaning; (b) schematic of the procedure with long interruption.

traditional methods like steam and autoclave curing. Unlike these conventional methods, which require high energy consumption and large-scale equipment, microwave curing provides rapid and uniform heating directly to the concrete mass, thereby accelerating the hydration process more efficiently. The use of microwaves generates heat internally, which reduces thermal gradients and potential cracking caused by uneven temperature distribution. Additionally, microwave curing can be integrated seamlessly with the extrusion process in printcrete, allowing for real-time active control of the material's properties and enabling immediate hardening upon extrusion, which has been tried for printcrete [64].

Despite its advantages, the application of microwave curing still has several challenges. The high cost of microwave equipment, the need for specialized training for operators, and safety concerns related to the handling of microwave radiation pose significant barriers to widespread commercial adoption. For instance, workers must be trained to operate microwave curing equipment safely to avoid exposure to high-intensity electromagnetic fields, which can pose health risks. Moreover, the initial setup costs for microwave curing systems are substantially higher compared to traditional methods, which may deter some construction firms from adopting this technology despite its long-term benefits.

6 Discussion and perspectives

Printcrete emerges as an innovative alternative to conventional shotcrete for tunnel engineering, offering distinct advantages such as no rebound and greater flexibility. This paper provides a summary of the previous studies on printcrete conducted by the authors. Furthermore, it offers an in-depth review and forward-looking perspective on the future development of printcrete. In this last section, we further emphasize critical considerations, focusing on three interconnected aspects across different sections, including upscaling, performance, and smart construction of printcrete.

The upscaling of printcrete is essential to improving the construction efficiency and sustainability of printcrete, which involves addressing challenges related to material formulation, testing, and equipment design. As discussed in Section 2, larger aggregates can enhance packing density, thus reducing the binder content required. However, this modification impacts various aspects of material performance. For instance, during pumping and extrusion, the inclusion of coarse aggregates influences flowability and increases the risk of clogging, particularly for inline mixing strategies with limited chamber sizes and remarkably accelerated reaction rates. Additionally, for the buildability discussed in Section 3, including coarse aggregates can negatively impact adhesion to the substrate as the presence of coarse aggregates may lead to larger air voids at the interface, particularly when the substrate surface is rough. From a testing and construction perspective, as detailed in Sections 4 and 5, it is essential to upscale both the testing setups and equipment to accommodate mixtures containing coarse aggregates. This is because the test configurations and processing chambers need to be appropriately designed to align with the maximum aggregate size, ensuring accurate performance evaluation and efficient material processing.

The performance of printcrete must account for its unique requirements, including pumpability, extrudability, buildability, and structural ability, as detailed in Section 3. One of the biggest challenges is balancing the conflicting demands of pumpability and buildability, in which the material must be fluid enough for efficient pumping while quickly gaining sufficient strength immediately after extrusion to provide early-age support for surrounding rocks. To tackle this challenge, the twin-pipe pumping technology developed by the authors has demonstrated its effectiveness, enabling printcrete to achieve its initial setting within a few minutes after extrusion. Consequently, conventional testing methods fall short in accurately characterizing the time-dependent properties of printcrete. As discussed in Section 4, there is a pressing need to develop new indices and standardized testing methods that can capture the continuous changes in hydration and rheology of printcrete in its early age. Furthermore, existing characterization methods are often too impractical for on-site application, highlighting the necessity of rapid detection techniques that integrate seamlessly into the construction process (Section 5).

The smart construction of printcrete is particularly crucial in extreme environments, such as geothermal zones or cold regions, where human intervention is challenging or impossible. Automated systems not only ensure safety but also enhance precision and efficiency in these demanding conditions. Smart equipment is essential for achieving fully automated construction processes, enabling real-time adaptation to changes in external environmental conditions or internal material states. Thus, a thorough understanding of the interaction between environmental factors and printcrete properties is essential, along with insights into the flow behavior influenced by hydration kinetics, as detailed in Sections 2 and 3. This includes studying the hydration kinetics of different binder phases under varying temperature conditions, as well as the evolution of rheological properties during different stages of the printing process. Advanced smart devices, integrated with AI capabilities, play a crucial role in real-time monitoring and decision-making, as highlighted in Section 5.

Acknowledgements The authors acknowledge the financial support provided by the Ministry of Science and Technology of China (No.

2021YFE0114100), the Science and Technology Commission of Shanghai Municipality (No. 23DZ1202906), the Major Engineering Science and Technology Project of Jiangxi Provincial Department of Transportation (No. 2021C0008), and the ETH Zurich Postdoctoral Fellowship (No. 23-2 FEL-059).

Funding note Open access funding provided by Swiss Federal Institute of Technology Zurich

Open Access This article is licensed under a Creative Commons Attribution 4.0 International License (https://creativecommons.org/licenses/by/4.0/), which permits use, sharing, adaptation, distribution and reproduction in any medium or format, as long as you give appropriate credit to the original author(s) and the source, provide a link to the Creative Commons license, and indicate if changes were made. The images or other third party material in this article are included in the article's Creative Commons license, unless indicated otherwise in a credit line to the material. If material is not included in the article's Creative Commons license and your intended use is not permitted by statutory regulation or exceeds the permitted use, you will need to obtain permission directly from the copyright holder. To view a copy of this license, visit http://creativecommons.org/licenses/by/4.0/.

Competing interests The authors declare that they have no competing interests.

References

1. Khoshnevis B. Automated construction by contour crafting—Related robotics and information technologies. Automation in Construction, 2004, 13(1): 5–19
2. de Schutter G, Lesage K, Mechtcherine V, Nerella V N, Habert G, Agusti-Juan I. Vision of 3D printing with concrete—Technical, economic and environmental potentials. Cement and Concrete Research, 2018, 112: 25–36
3. Yuan Y, Wang X Y, Tao Y X. Bond properties between printable concrete and rock. In: Proceedings of the 5th International fib Congress. Melbourne: fib Congress, 2018
4. Tao Y X. Automated Construction and Structural Behavior of 3D Printed Concrete Tunnel Linings. Dissertation for the Doctoral Degree. Ghent: Ghent University, 2021
5. Vantyghem G, Ooms T, de Corte W. VoxelPrint: A Grasshopper plug-in for voxel-based numerical simulation of concrete printing. Automation in Construction, 2021, 122: 103469
6. Liu Y, Wang L, Yuan Q, Peng J W. Effect of coarse aggregate on printability and mechanical properties of 3D printed concrete. Construction and Building Materials, 2023, 405: 133338
7. Wangler T, Patankar Y, Flatt R J. Sustainable digital concrete: Myth, reality or emerging opportunity? Architectural Design, 2024, 94(5): 22–29
8. Wangler T, Tao Y X, Das A, Mahmoudi M, Gürel S, Flatt R J. Aluminate 2K systems in digital concrete: Process, design, chemistry, and outlook. Cement and Concrete Research, 2024, 185: 107644
9. Mohan M K, Rahul A V, van Dam B, Zeidan T, de Schutter G, van Tittelboom K. Performance criteria, environmental impact and cost assessment for 3D printable concrete mixtures. Resources, Conservation and Recycling, 2022, 181: 106255
10. Ren Q, Tao Y X, Jiao D W, de Schutter G, Jiang Z W. Rheological properties of concrete with manufactured sand: A multi-level prediction. Cement and Concrete Composites, 2022, 133: 104647
11. Tao Y X, Ren Q, Lesage K, van Tittelboom K, Yuan Y, de Schutter G. Shape stability of 3D printable concrete with river and manufactured sand characterized by squeeze flow. Cement and Concrete Composites, 2022, 133: 104674
12. Luo Q, Liu P F, Wu M. Re-using excavated rock from underground tunneling activities to develop eco-friendly ultrahigh performance concrete. Case Studies in Construction Materials, 2024, 20: e02867
13. Yuan Y, Fatoyinbo I O, Sheng R Y, Wang Q L, Zia S M M, Cui P Y, Zhang J L. Advancing the applicability of recycled municipal solid waste incineration bottom ash as a cement substitute in printable concrete: Emphasis on rheological and microstructural properties. Journal of Building Engineering, 2025, 103: 112133
14. Zia S M M, Yuan Y, Irfan-ul-Hassan M, Sheng R Y, Fatoyinbo I O, Wang Q L, Zhang J L. Influence of sugarcane bagasse ash on the workability and mechanical behaviour of 3D-printed mortar. Low-Carbon Materials and Green Construction, 2026, 4(1): 4
15. Han J G, Wang K J, Wang Y, Shi J Y. Study of aluminum sulfate and anhydrite on cement hydration process. Materials and Structures, 2016, 49(4): 1105–1114
16. Pang X Y, Bentz D P, Meyer C, Funkhouser G P, Darbe R. A comparison study of Portland cement hydration kinetics as measured by chemical shrinkage and isothermal calorimetry. Cement and Concrete Composites, 2013, 39: 23–32
17. Mohan M K, Rahul A V, Tao Y X, de Schutter G, van Tittelboom K. Hydration re-initiation of borated CSA systems with a two-stage mixing process: An application in extrusion-based concrete 3D printing. Cement and Concrete Research, 2022, 159: 106870
18. Tao Y X, Mohan M K, Rahul A V, de Schutter G, van Tittelboom K. Hydration and microstructure of calcium sulfoaluminate-Portland cement binder systems for set-on-demand applications. Materials and Structures, 2024, 57(2): 35
19. Tao Y X, Zhang Y, de Schutter G, van Tittelboom K. Interfacial bonding of 3D printable concrete with chemically reactive coating for automatic repair. Developments in the Built Environment, 2024, 17: 100333
20. Tao Y X, Mohan M K, Rahul A V, de Schutter G, van Tittelboom K. Development of a calcium sulfoaluminate-Portland cement binary system for twin-pipe 3D concrete printing. Cement and Concrete Composites, 2023, 138: 104960
21. Das A, Reiter L, Mantellato S, Flatt R J. Early-age rheology and hydration control of ternary binders for 3D printing applications. Cement and Concrete Research, 2022, 162: 107004
22. Tao Y X, Dai X D, de Schutter G, van Tittelboom K. Set-on-demand of alkali-activated slag mixture using twin-pipe pumping. Construction and Building Materials, 2023, 392: 132003
23. Sun Y B, Mohan M K, Tao Y X, Zhang Y, van Tittelboom K, Ye G, de Schutter G. A conceptual design of two-stream alkali-activated materials. Cement and Concrete Composites, 2024, 148: 105485

24. Özalp F. Mechanical behavior and permeability properties of sustainable and high-performance anisotropic three-dimensional printable concrete. Frontiers of Structural and Civil Engineering, 2023, 17(11): 1662–1674
25. Roussel N, Lanos C. Plastic fluid flow parameters identification using a simple squeezing test. Applied Rheology, 2003, 13(3): 132–141
26. Tao Y X, Zhou J G, Cui W J, Shi X Y, de Schutter G, van Tittelboom K. Numerical assessment of plastic yielding in extrusion-based 3D concrete printing. Materials and Structures, 2024, 57(4): 65
27. Suiker A S J, Wolfs R J M, Lucas S M, Salet T A M. Elastic buckling and plastic collapse during 3D concrete printing. Cement and Concrete Research, 2020, 135: 106016
28. Tao Y X, Lesage K, van Tittelboom K, Yuan Y, de Schutter G. Influence of aluminum sulfate on mobility and adhesion of hydroxyethyl methyl cellulose in cement-based materials for tunnel linings. Cement and Concrete Composites, 2022, 131: 104594
29. Tao Y X, Lesage K, van Tittelboom K, Yuan Y, de Schutter G. Influence of substrate surface roughness and moisture content on tensile adhesion performance of 3D printable concrete. Cement and Concrete Composites, 2022, 126: 104350
30. Tao Y X, Vantyghem G, Lesage K, Yuan Y, de Corte W, van Tittelboom K, de Schutter G. Adhesion properties of printable polymer-modified concrete for rock tunnel linings. ACI Materials Journal, 2021, 118(6): 61–73
31. Tao Y X, Ren Q, Vantyghem G, Lesage K, van Tittelboom K, Yuan Y, de Corte W, de Schutter G. Extending 3D concrete printing to hard rock tunnel linings: Adhesion of fresh cementitious materials for different surface inclinations. Automation in Construction, 2023, 149: 104787
32. Roussel N. Rheological requirements for printable concretes. Cement and Concrete Research, 2018, 112: 76–85
33. Li R H, Yuan Y, Zhao X, Bilotta E, Huang J Q. Local site effect of fault site and its impact on seismic response of fault-crossing tunnel. Journal of Earthquake Engineering, 2024, 28(11): 3019–3037
34. Zhang S H, Yuan Y, Yang Y S, Li C, Yu H T. Experimental investigation of seismic performance of segmental tunnel with secondary lining under strong earthquake. Structures, 2024, 60: 105833
35. Cicione A, Kruger J, Walls R S, van Zijl G. An experimental study of the behavior of 3D printed concrete at elevated temperatures. Fire Safety Journal, 2021, 120: 103075
36. Suntharalingam T, Gatheeshgar P, Upasiri I, Poologanathan K, Nagaratnam B, Corradi M, Nuwanthika D. Fire performance of innovative 3D printed concrete composite wall panels—A numerical study. Case Studies in Construction Materials, 2021, 15: e00586
37. Engmann J, Servais C, Burbidge A S. Squeeze flow theory and applications to rheometry: A review. Journal of Non-Newtonian Fluid Mechanics, 2005, 132(1–3): 1–27
38. Huang T J, Li B Y, Yuan Q, Shi Z G, Xie Y J, Shi C J. Rheological behavior of Portland clinker-calcium sulphoaluminate clinker-anhydrite ternary blend. Cement and Concrete Composites, 2019, 104: 103403
39. Mohan M K, Rahul A V, van Tittelboom K, de Schutter G. Rheological and pumping behaviour of 3D printable cementitious materials with varying aggregate content. Cement and Concrete Research, 2021, 139: 106258
40. Yuan Y, Wang X Y, Chen X, Xiao P, Koenders E, Dai Y. Mathematical models of apparent viscosity as a function of water–cement/binder ratio and superplasticizer in cement pastes. Scientific Reports, 2023, 13(1): 22301
41. Roussel N, Ovarlez G, Garrault S, Brumaud C. The origins of thixotropy of fresh cement pastes. Cement and Concrete Research, 2012, 42(1): 148–157
42. Jiao D W, Lesage K, Yardimci M Y, El Cheikh K, Shi C J, de Schutter G. Structural evolution of cement paste with nano-Fe_3O_4 under magnetic field—Effect of concentration and particle size of nano-Fe_3O_4. Cement and Concrete Composites, 2021, 120: 104036
43. Tao Y X, Mohan M K, Rahul A V, de Schutter G, van Tittelboom K. Influence of rheology on mixing homogeneity and mechanical behavior of twin-pipe 3D printable concrete. Construction and Building Materials, 2023, 408: 133694
44. Ye G, Lura P, van Breugel K, Fraaij A L A. Study on the development of the microstructure in cement-based materials by means of numerical simulation and ultrasonic pulse velocity measurement. Cement and Concrete Composites, 2004, 26(5): 491–497
45. Benaicha M, Jalbaud O, Hafidi Alaoui A, Burtschell Y. Correlation between the mechanical behavior and the ultrasonic velocity of fiber-reinforced concrete. Construction and Building Materials, 2015, 101: 702–709
46. Pan T H, Guo R X, Jiang Y Q, Ji X P. How do the contact surface forces affect the interlayer bond strength of 3D printed mortar? Cement and Concrete Composites, 2022, 133: 104675
47. Yuan Y, Wang X Y, Zhang J L, Tao Y X, van Tittelboom K, Taerwe L, de Schutter G. The shear strength of the interface between artificial rock and printed concrete at super-early ages. Frontiers of Structural and Civil Engineering, 2024, 18(1): 51–65
48. Parente L, Falvo E, Castagnetti C, Grassi F, Mancini F, Rossi P, Capra A. Image-based monitoring of cracks: Effectiveness analysis of an open-source machine learning-assisted procedure. Journal of Imaging, 2022, 8(2): 22
49. Sheng R Y, Yuan Y, Zhang J Y, Liu Y Q, Yao X P, Tao Y X, Zhang J L. An interpretable multimodal monitoring system for mixing process of printcrete: Integrating computer vision, torque, and temperature. Cement and Concrete Composites, 2026, 172: 106685
50. de Schryver R. Active rheology control of cementitious materials: Numerical and experimental pumping investigation. Dissertation for the Doctoral Degree. Ghent: Ghent University, 2022
51. Guo B Y, Liu X H, Tan X H. Hydraulic fracturing. In: Guo B Y, Liu X H, Tan X H, eds. Petroleum Production Engineering. 2nd ed. Boston: Gulf Professional Publishing, 2017, 389–501
52. Kwon S H, Jang K P, Kim J H, Shah S P. State of the art on prediction of concrete pumping. International Journal of Concrete Structures and Materials, 2016, 10(3): 75–85
53. Tao Y X, Rahul A V, Mohan M K, van Tittelboom K, Yuan Y, de Schutter G. Blending performance of helical static mixer used for twin-pipe 3D concrete printing. Cement and Concrete Composites,

2022, 134: 104741

54. Oddie G, Pearson J R A. Flow-rate measurement in two-phase flow. Annual Review of Fluid Mechanics, 2004, 36: 149–172
55. Krishna S, Thonhauser G, Kumar S, Elmgerbi A, Ravi K. Ultrasound velocity profiling technique for in-line rheological measurements: A prospective review. Measurement, 2022, 205: 112152
56. Tan C, Murai Y, Liu W L, Tasaka Y, Dong F, Takeda Y. Ultrasonic doppler technique for application to multiphase flows: A review. International Journal of Multiphase Flow, 2021, 144: 103811
57. Reiter L, Wangler T, Anton A, Flatt R J. Setting on demand for digital concrete—Principles, measurements, chemistry, validation. Cement and Concrete Research, 2020, 132: 106047
58. Tao Y X, Mohan M K, Rahul A V, Yuan Y, de Schutter G, van Tittelboom K. Stiffening controllable concrete modified with redispersible polymer powder for twin-pipe printing. Cement and Concrete Research, 2022, 161: 106953
59. Tao Y X, Lesage K, van Tittelboom K, Yuan Y, de Schutter G. Twin-pipe pumping strategy for stiffening control of 3D printable concrete: From transportation to fabrication. Cement and Concrete Research, 2023, 168: 107137
60. Tao Y X, Rahul A V, Mohan M K, de Schutter G, van Tittelboom K. Enhancing mechanical performance of twin-pipe printable concrete using a binary binder system. Materials Letters, 2023, 346: 134515
61. Deetman A, Bos D, Blaakmeer J, Salet T, Lucas S. An in-line dye tracer experiment to measure the residence time in continuous concrete processing. Materials and Structures, 2024, 57(5): 104
62. Khunt Y, Nathwani V, Patel H, Joshi T, Gandhi D. Investigation on properties of autoclave aerated concrete using different pre-curing and curing techniques. Materials Today: Proceedings, 2023,
63. Wang W Z, Shen A Q, Zhou J L, Cang Y J, Zhang X M, Tong Y Y. Shrinkage evolution and mechanism of self-curing concrete cooperatively cured with superabsorbent polymers and waterborne epoxy coatings. Journal of Building Engineering, 2024, 96: 110606
64. Ma G W, Sun J B, Wang L, Aslani F, Liu M. Electromagnetic and microwave absorbing properties of cementitious composite for 3D printing containing waste copper solids. Cement and Concrete Composites, 2018, 94: 215–225